JACS
JOURNAL OF THE AMERICAN CHEMICAL SOCIETY
Article
Cite This: J. Am. Chem. Soc. 2018, 140, 4596−4603
pubs.acs.org/JACS

Fine Tuning and Specific Binding Sites with a Porous Hydrogen-Bonded Metal-Complex Framework for Gas Selective Separations

Zongbi Bao,[†] Danyan Xie,[†] Ganggang Chang,[†,⊥] Hui Wu,[§] Liangying Li,[†] Wei Zhou,*[,§] Hailong Wang,[‡] Zhiguo Zhang,[†] Huabin Xing,[†] Qiwei Yang,[†] Michael J. Zaworotko,[¶] Qilong Ren,*[,†] and Banglin Chen*[,‡]

[†]Key Laboratory of Biomass Chemical Engineering of Ministry of Education, College of Chemical and Biological Engineering, Zhejiang University, Hangzhou 310027, P.R. China

[‡]Department of Chemistry, University of Texas at San Antonio, One UTSA Circle, San Antonio, Texas 78249-0698, United States

[§]NIST Center for Neutron Research, National Institute of Standards and Technology, Gaithersburg, Maryland 20899-6102, United States

[⊥]School of Chemistry, Chemical Engineering and Life Sciences, Wuhan University of Technology, Wuhan 430070, P.R. China

[¶]Department of Chemical and Environmental Sciences, University of Limerick, Limerick V94 T9PX, Republic of Ireland

Supporting Information

ABSTRACT: Research on hydrogen-bonded organic frameworks (HOFs) has been developed for quite a long time; however, those with both established permanent porosities and functional properties are extremely rare due to weak hydrogen-bonding interactions among molecular organic linkers, which are much more fragile and difficult to stabilize. Herein, through judiciously combining the superiority of both the moderately stable coordination bonds in metal−organic frameworks and hydrogen bonds, we have realized a microporous hydrogen-bonded metal-complex or metallotecton framework HOF-21, which not only shows permanent porosity, but also exhibits highly selective separation performance of C_2H_2/C_2H_4 at room temperature. The outstanding separation performance can be ascribed to sieving effect confined by the fine-tuning pores and the superimposed hydrogen-bonding interaction between C_2H_2 and SiF_6^{2-} on both ends as validated by both modeling and neutron powder diffraction experiments. More importantly, the collapsed HOF-21 can be restored by simply immersing it into water or salt solution. To the best of our knowledge, such extraordinary water stability and restorability of HOF-21 were observed for the first time in HOFs, underlying the bright perspective of such new HOF materials for their industrial usage.

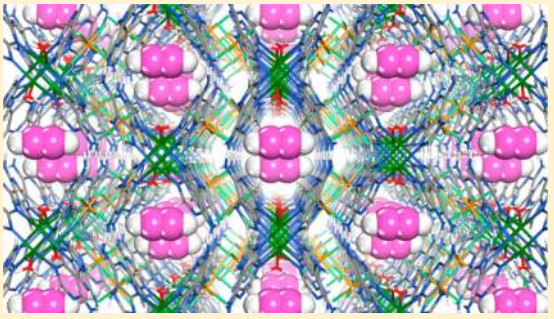

INTRODUCTION

Novel porous materials have the promise to gradually weed out the traditional costly and energy-intensive technologies, such as amine scrubbing and cryogenic distillation, through the adsorption-based gas separations.[1] Over the past two decades, extensive research endeavors on porous materials have eventually led to the emergence of porous metal−organic frameworks (MOFs)[2] and covalent−organic frameworks (COFs),[3] whose separation selectivities and capacities have surpassed those traditional zeolite materials for some important gas separations. Compared with MOFs and COFs, which are self-assembled through coordination and covalent bonding of their corresponding building units, hydrogen-bonded organic frameworks (HOFs), self-assembled frameworks by utilizing intermolecular hydrogen-bonding interactions, have recently been realized as potential porous materials as well. Although their porosities might be not as high as those of MOFs and COFs, HOFs are superior to MOFs and COFs because of their facile synthesis and characterization as well as easy purification and regeneration by simple soaking.[4] Furthermore, high porosities of porous materials are not the prerequisites for their gas separation applications. In fact, most porous materials exhibiting excellent performance for gas separations are those of moderate porosities with Brunauer−Emmett−Teller (BET) surface areas less than 1000 m^2/g, which means that HOFs are very promising candidates for gas separations. Indeed, a few HOFs have been established for their gas separations. Because hydrogen bonding interactions are much weaker than coordination and covalent bonds, it is still very challenging to stabilize the HOFs in which most frameworks collapsed during the framework activations.

Current research on HOFs has been mainly focused on the usage of pure organic linkers or building blocks. As demonstrated in the development of mixed metal−organic frameworks (M'MOFs),[5] incorporation of metal-complexes or

Received: December 27, 2017
Published: March 14, 2018

DOI: 10.1021/jacs.7b13706
J. Am. Chem. Soc. 2018, 140, 4596−4603

metallotectons into the porous materials can readily generate unique pore structures, topologies, and functionalities; however, HOFs with metal-complexes as the building units have been rarely explored.[6] The usage of $[Cu_2(ade)_4]$ (ade= adenine) to construct porous HOFs by Zaworotko group,[6b] as exemplified by $[Cu_2(ade)_4]\cdot 2TiF_6$ (MPM-1-TIFSIX), has attracted great interest. Such a simple metal-complex strategy has not only opened a new methodology to construct porous HOFs in which some unconventional organic linkers can be readily assembled into the porous materials, but also provided diverse ways to tune and functionalize the pores through the deliberate choices of metal clusters and the accessible sites on the metal centers. Herein we report a novel HOF assembled from $[Cu_2(ade)_4]$ with the cosupporting SiF_6^{2-} anions. To our great surprise, the resulting HOF $[Cu_2(ade)_4(H_2O)_2]\cdot 2SiF_6$ (termed HOF-21) has a significantly different structure from MPM-1-TIFSIX because of the occupancy of water molecules on the copper sites in HOF-21. Accordingly, the HOF-21 has a smaller pore sizes of 3.6 Å than MPM-1-TIFSIX of 7.1 Å Furthermore, the specific binding sites of SiF_6^{2-} on the pore surfaces further induce their preferential recognition of C_2H_2 molecules. Thus, HOF-21 exhibits much higher and efficient C_2H_2/C_2H_4 separation properties than MPM-1-TIFSIX, as clearly demonstrated by breakthrough experiments. Neutron diffraction studies and density functional theory (DFT) calculations further confirm the recognition mechanisms. HOF-21 shows exceptionally high stability and can be easily regenerated through simple soaking in the water.

EXPERIMENTAL SECTION

All reagents and solvents were used as received without any purification. Powder X-ray diffraction (PXRD) patterns of the samples were recorded with a XPert diffractometer (Panalytical Corp., Netherlands) using Cu Ka (λ = 0.1543 nm) radiation at 40 kV from 5° to 40° (2θ angle range) with a scanning step size of 0.02°. Thermogravimetric analysis (TGA) of HOF-21 was performed at a heating rate of 10 °C/min under a nitrogen flow on a thermogravimetric analyzer Pyris-1 TGA (PerkinElmer, USA). Infrared spectra were obtained using a Fourier transform infrared spectroscopy Nicolet iS10 (Thermo Fisher Scientific Inc., USA). Elemental analysis (EA) was carried out on Vario MICRO Elemental Analyzer (Elementar Company, Germany).

Preparation of $[Cu_2(ade)_4(H_2O)_2](SiF_6)_2$ (HOF-21). At room temperature, 0.152 mmol (20.5 mg) of adenine dissolved in 3 mL of 1:1 acetonitrile/H_2O was layered above 3 mL of an aqueous solution containing 0.076 mmol (17.75 mg) of $Cu(NO_3)_2\cdot 3H_2O$ and 0.076 mmol (13.53 mg) of $(NH_4)_2SiF_6$. One milliliter of 1:1 acetonitrile/H_2O was layered between the top and bottom solutions to slow the rate of reaction. Dark blue, rectangular prismatic crystals formed in 30% yield (based on the weight of HOF-21a) after 4 days. These crystals were suitable for structure resolution by single-crystal X-ray crystallography. Unless indicated otherwise, this synthetic methodology was used to prepare sample for gas sorption measurements and breakthrough experiments. IR (KBr pellet): 3131 (m), 1658 (s), 1625 (m), 1605 (m), 1589 (w), 1459 (s), 1411 (s), 1351 (w), 1316 (s), 1236 (s), 1179 (w), 1029 (m), 970 (w), 936 (w), 788 cm^{-1} (m); elemental analysis calcd (%) for $[Cu_2(ade)_4(H_2O)_2](SiF_6)_2$: C 24.30, H 2.43, N 28.34; found 24.21, H 2.56, N 28.27.

Activation of HOF-21 (Denoted as HOF-21a). The as-synthesized HOF-21 was exchanged with fresh methanol several times to displace water molecules and then evacuated under dynamic vacuum at 298 K for 24 h to obtain activated HOF-21 before confirming the porosity.

Restoration of framework-collapsed HOF-21a. The pore structure of HOF-21a collapsed when it was evacuated under dynamic vacuum at temperature of 423 K. The collapsed frameworks (~100 mg) were soaked into pure water (20 mL) or an aqueous solution (20 mL) containing $(NH_4)_2SiF_6$ (0.50 mmol, 89.0 mg) for 48 h. The regenerated frameworks were collected by centrifugation and then activated under a high vacuum at room temperature for 24 h prior to porosity measurements.

Single Crystal X-ray Diffraction of HOF-21. Single crystal X-ray diffraction data of as-synthesized HOF-21 were collected at 293 K on a Gemini A Ultra diffractometer graphite-monochromatic enhanced Mo radiation (λ = 0.71073). The structure was solved by direct methods and refined by full-matrix least-squares methods with the SHELXTL program package. The solvent molecules in as-synthesized HOF-21 crystal are highly disordered. The SQUEEZE subroutine of the PLATON software suite was used to remove the scattering from the highly disordered guest molecules. Single crystal X-ray diffraction revealed that HOF-21 crystallized in the orthorhombic space group *Cmcm* (see Table 1).

Table 1. Crystal Data and Structure Refinement for As-Synthesized HOF-21

identification code	HOF-21
empirical formula	$C_{20}H_{24}Cu_2F_{12}N_{20}O_2Si_2$
formula weight	987.85
temperature (K)	293 K
crystal system	orthorhombic
space group	*Cmcm*
cell	a = 16.9982 (8) Å, b = 11.0287 (5) Å, c = 21.3180 (11) Å
	α = 90°, β = 91.676°, γ = 90°
volume ($Å^3$)	3996.4(3)
Mu (mm^{-1})	1.231
ρ_{calc} (g cm^{-3})	1.642
Z	4
F000	1976.0
F000′	1980.24
h, k, l_{max}	20, 13, 25
N_{ref}	1953
T_{min}, T_{max}	0.633, 0.753
T_{min}'	0.620

Neutron Diffraction Experiment. Neutron powder diffraction data were collected using the BT-1 neutron powder diffractometer at the NIST Center for Neutron Research. A Ge(311) monochromator with a 75° takeoff angle, lambda = 2.0787(2) Å, and in-pile collimation of 60 min of arc were used. Data were collected over the range of 1.3–166.3° 2-Theta with a step size of 0.05°. Fully activated HOF-21a sample was loaded in a vanadium can equipped with a capillary gas line and a packless valve. A closed-cycle He refrigerator was used for sample temperature control. The bare HOF-21a sample was measured first at temperatures of 200 K. To probe the gas adsorption locations, a predetermined amount of C_2D_2 was loaded into the sample at room temperature (deuterated gas C_2D_2 was used to avoid the large incoherent neutron scattering background that would be produced by the hydrogen in C_2H_2). The sample was then slowly cooled to 200 K before diffraction data were collected. Rietveld structural refinements were performed on the diffraction data using the GSAS package.[7] Because of the large number of atoms in the crystal unit cell, the adenine ligand molecule and the gas molecule were both treated as rigid bodies in the Rietveld refinement (to limit the number of variables), with the molecule orientation and center of mass freely refined. Final refinement on the positions/orientations of the rigid bodies, thermal factors, occupancies, lattice parameters, background, and profiles converges with satisfactory R-factors.

Density Functional Theory Calculations. Our first-principles density functional theory (DFT) calculations were performed using the Quantum-Espresso package.[8] A semiempirical addition of dispersive forces to conventional DFT[9] was included in the calculation to account for van der Waals interactions. We used Vanderbilt-type

DOI: 10.1021/jacs.7b13706
J. Am. Chem. Soc. 2018, 140, 4596–4603

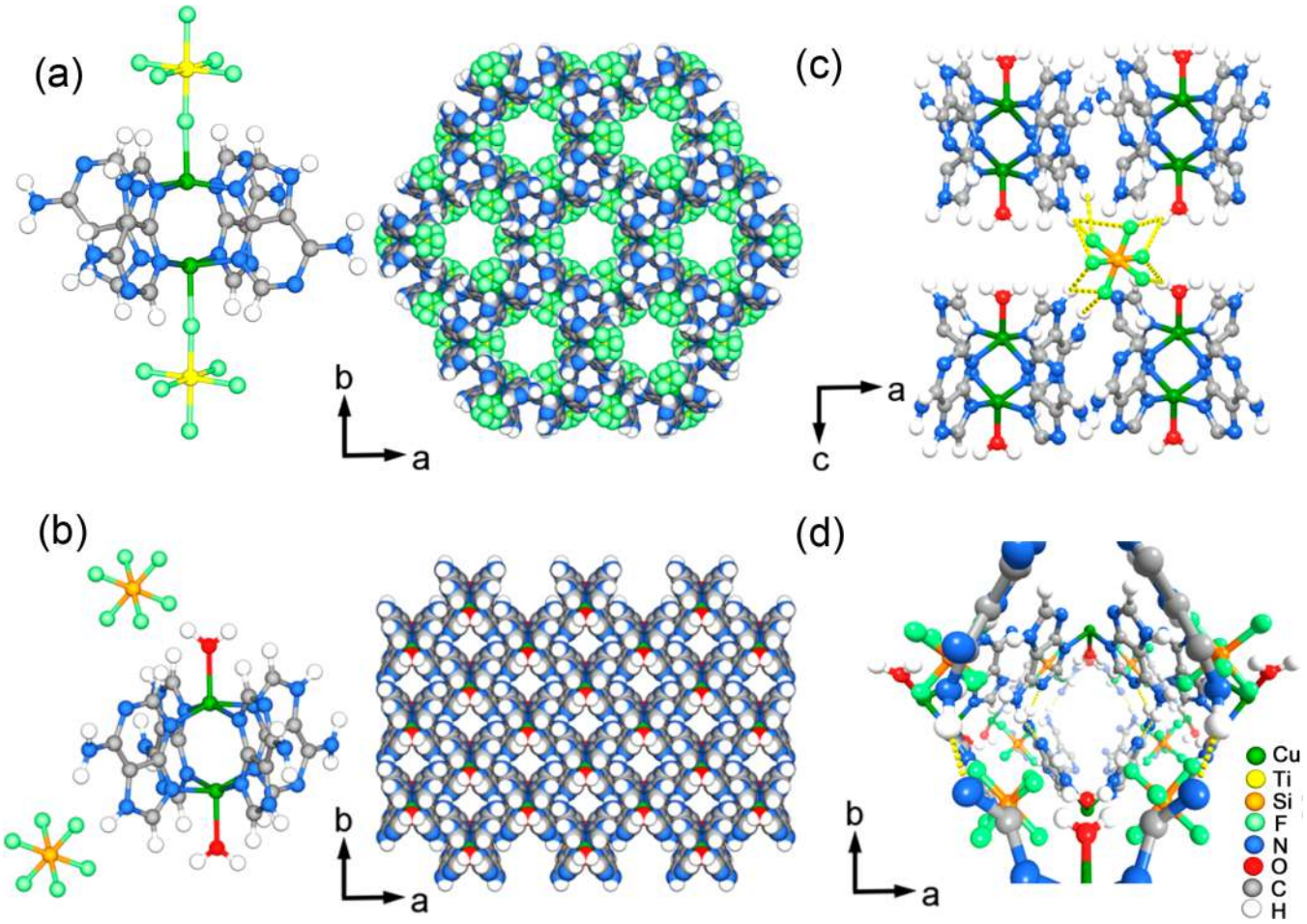

Figure 1. X-ray crystal structure of HOF-21. (a) Building block of MPM-1-TIFSIX, discrete dinuclear paddle-wheel ionic complex features four adenine ligands in equatorial positions and TiF^{2-} in axial positions, and 3D framework packing along the *c* axis showing the 1D channels of about 7.1 Å in diameter. (b) Building block of HOF-21, discrete dinuclear paddle-wheel ionic complex features four adenine ligands in equatorial positions and two water molecules in axial positions, and 3D framework packing along the *c* axis showing the 1D channels of about 3.6 Å in diameter. (c) Hydrogen-bonding interaction networks between the SiF_6^{2-} and the building blocks viewing along the *b* axis. (d) Hydrogen-bonding interactions among building blocks viewing along *c* axis in HOF-21. Cu, green; Si, orange; Ti, yellow; F, light green; N, blue; O, red; C, gray; H, white.

ultrasoft pseudopotentials and the generalized gradient approximation (GGA) with the Perdew–Burke–Ernzerof (PBE) exchange correlation. A cutoff energy of 544 eV and a 2 × 4 × 2 *k*-point mesh (generated using the Monkhosrt Pack scheme) were found to be enough for total energy to converge within 0.01 meV/atom.

We first optimized the HOF-21a structures. C_2H_2 gas molecule was then introduced to the optimized HOF structure at the experimentally identified adsorption site, followed by a full structural relaxation. To obtain the gas binding energy, a gas molecule placed in a supercell with the same cell dimensions was also relaxed as a reference. The static binding energy (at T = 0 K) was then calculated using $E_B = E$(HOF-21a) + E(gas_molecule) − E(HOF-21a + gas_molecule).

Gas Adsorption Measurements. Gas adsorption measurements were performed volumetrically in a Micromeritics ASAP 2050 adsorption apparatus. The adsorption isotherms were obtained at temperatures from 273 to 298 K and gas pressures from 0 to 826 mmHg. A roughly 150 mg sample prepared by the aforementioned synthesized methodology was used for the gas adsorption studies. The initial outgassing process was carried out under a vacuum at room temperature for 24 h. The free space of the system was determined by using the helium gas. The degas procedure was repeated on the same sample between measurements for 12 h. Ultrahigh purity grade helium (99.999%), acetylene (>99%), ethylene (99.99%), carbon dioxide (99.99%), and nitrogen (99.99%) were purchased from Jingong Co., Ltd. (China).

Column Breakthrough Experiments. In a typical experiment, 793.3 mg of HOF-21a (or 687.3 mg of MPM-1-TIFSIX) ground powder was packed into a column (4.6 mm I.D. × 50 mm). The HOF-21 and MPM-1-TIFSIX sorbents were activated in Micromeritics ASAP 2050 adsorption apparatus at 298 K under high dynamic vacuum (6 μmHg), respectively. Column packing was conducted in glovebox filled with Argon. A helium flow (5 cm^3/min) was introduced into the column to further purge the adsorbent. The flow of helium was then turned off while a gas mixture of C_2H_2/C_2H_4 (50:50, *v*/*v*) at 0.20 cm^3/min was allowed to feed into the column.

■ RESULTS AND DISCUSSION

A slow diffusion of adenine solution into the mixed solution of $Cu(NO_3)_2{\cdot}3H_2O$ and $(NH_4)_2SiF_6$ at room temperature for 4 days yielded the deep blue rectangular prismatic single crystals of HOF-21. The phase purity of HOF-21 was well confirmed by matching the experimental and simulated powder X-ray diffraction patterns (see Figure S1) and TGA (see Figure S2) and EA studies. Single crystal X-ray diffraction revealed that HOF-21 crystallized in the orthorhombic space group *Cmcm* (see Table 1). As shown in Figure 1b–d, HOF-21 has a significantly different structure from MPM-1-TIFSIX (Figure 1a). HOF-21 is assembled from a discrete dinuclear paddle-wheel ionic complex $[Cu_2(ade)_4(H_2O)_2]^{4+}$ in which the

DOI: 10.1021/jacs.7b13706
J. Am. Chem. Soc. 2018, 140, 4596–4603

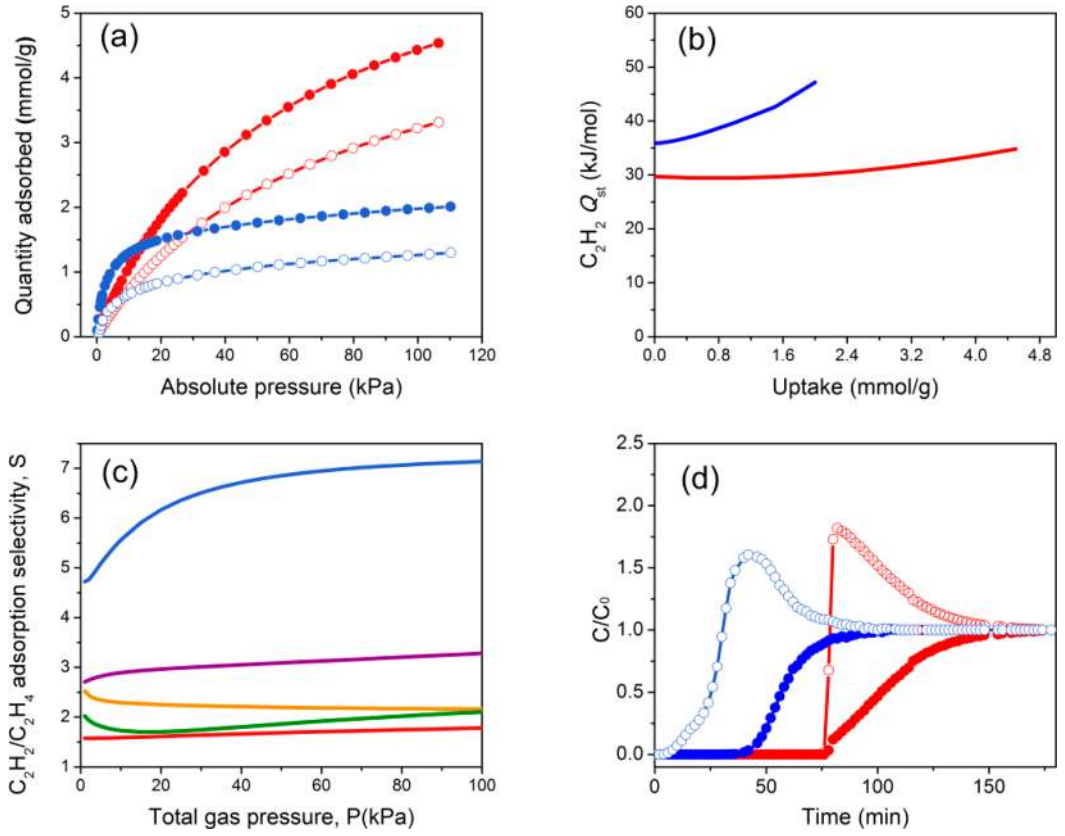

Figure 2. Experimental adsorption properties and breakthrough curves of HOF-21a and MPM-1-TIFSIX for C_2H_2/C_2H_4 separation. (a) Adsorption isotherms of C_2H_2 (solid) and C_2H_4 (hollow) on HOF-21a (blue) and MPM-1-TIFSIX (red) at 298 K. (b) Q_{st} of C_2H_2 by fitting isotherms obtained at 298 and 273 K to the Virial equation on HOF-21a (blue) and MPM-1-TIFSIX (red). (c) IAST selectivity for 50:50 C_2H_2/C_2H_4 binary mixture of HOF-21a (blue) and the other four materials including M'MOF-2a (purple), MgMOF-74 (orange), NOTT-300a (green), and MPM-1-TIFSIX (red) at 298 K. (d) Experimental column breakthrough curves for 50:50 C_2H_2/C_2H_4 binary mixture at 298 K and 1 bar in an adsorber bed packed with HOF-21a (blue) or MPM-1-TIFSIX (red). Hollow dot is for C_2H_4, and solid dot is for C_2H_2.

counterions of SiF_6^{2-} are not coordinated to the Cu^{2+}. In the structure of MPM-1-TIFSIX, the two axial positions of the Cu^{2+} center are occupied by the TiF_6^{2-} ions, while in HOF-21, two water molecules occupy these two axial positions. These $[Cu_2(ade)_4(H_2O)_2]^{4+}$ units self-assemble into a supramolecular ribbon chain, and then connect by multiple hydrogen bonding interactions between the $[Cu_2(ade)_4(H_2O)_2]^{4+}$ and SiF_6^{2-} segments to form a two-dimensional layer in *ab* plane, which further links with SiF_6^{2-} via the hydrogen bonding to generate an extrinsically porous hydrogen-bonding framework (see Figure 1c,d). Besides, there is partial $\pi-\pi$ stacking interaction between paralleled pyrimidine ring (see Figure 1b), which is also absent in MPM-1-TIFSIX. As shown in Figure 1b, HOF-21 contains one-dimensional channels of about 3.6 Å in diameter paralleled to the *c* axis, which are much smaller than the pore channels of about 7.1 Å in MPM-1-TIFSIX. It is noteworthy that such alteration of ligands in axial positions in HOF-21 compared with MPM-1-TIFSIX (TiF_6^{2-}) results in a significant difference in their connection style, especially the additional multiple hydrogen-bonding interactions between the $[Cu_2(ade)_4(H_2O)_2]^{4+}$ and SiF_6^{2-} segments, which might enhance the stability of HOF-21.

The porous nature of HOF-21 revealed by crystal structure encouraged us to investigate its permanent porosity using gas adsorption experiments. First, the as-synthesized HOF-21 was exchanged with methanol several times and then evacuated under dynamic vacuum at 298 K to obtain activated HOF-21 (denoted as HOF-21a), which does not uptake any N_2 gas molecules at 77 K (see Figure S3). Such phenomenon has been also observed in some microporous MOFs and HOFs, and a possible explanation is that the strong interactions between N_2 and the channel windows at 77 K hinder its diffusion into HOF-21.[10] In this case, it might arise from the diffusion resistance because of pore size comparable to the kinetic size of nitrogen molecules. However, the CO_2 gas sorption isotherm of HOF-21a at 196 K clearly indicates its microporous nature with a moderate BET surface area of 339.0 m^2/g (see Figure S3).

The establishment of permanent microporosity in HOF-21a prompted us to examine its performance in gas separation especially for the industrially important C_2H_2/C_2H_4 separation and compare with MPM-1-TIFSIX. MPM-1-TIFSIX (Figure 2a, red) takes up a larger amount of C_2H_2 and C_2H_4 over 25 kPa than HOF-21a (Figure 2a, blue) because of its higher porosity; however, under low pressure below 25 kPa, HOF-21a takes up much more C_2H_2 than MPM-1-TIFSIX. More importantly, HOF-21a takes up a much different amount of C_2H_2 and C_2H_4 at room temperature than MPM-1-TIFSIX, which means that HOF-21a exhibits much higher C_2H_2/C_2H_4 separation selectivity than MPM-1-TIFSIX. The gas uptake of C_2H_2 for HOF-21a is 1.98 mmol/g at 298 K and 1 bar, while the corresponding uptake of C_2H_4 is 1.27 mmol/g (see Figure 2a). Apparently, HOF-21a has much higher sieving effects because of its narrower pore for the separation of C_2H_2/C_2H_4. The weakly basic nature of SiF_6^{2-} also plays the roles for the

DOI: 10.1021/jacs.7b13706
J. Am. Chem. Soc. 2018, 140, 4596−4603

preferential binding of C_2H_2 over C_2H_4.[11] To understand the binding energy at low coverage, isosteric adsorption heats of C_2H_2 for HOF-21a are calculated using Virial equation (see Table S2). As shown in Figure 2b, the initial value of Q_{st} for C_2H_2 in HOF-21a is in the range of 36−47 kJ/mol (line blue), which is higher than those of MPM-1-TIFSIX (30−35 kJ/mol) (line red) and even comparable to those of MOFs with open metal sites,[12] indicating the relatively strong interactions between the guest C_2H_2 molecules and host HOF-21a framework. The increase of Q_{st} with increasing gas loading can probably be attributed to the intermolecular interaction of acetylene molecules. To further investigate the adsorption selectivity of HOF-21a and MPM-1-TIFSIX for equimolar binary mixture of C_2H_2/C_2H_4 (50:50, *v*/*v*), we performed calculations using the ideal adsorbed solution theory (IAST) with the fitted isotherms of the experimental data (Table S1). As shown in Figure 2c, at 298 K and 100 kPa, the adsorption selectivity of HOF- 21a (7.1) is comparable to that of UTSA-100a (7.4) and significantly higher than those of examined MOFs during the whole pressure range, including MMOF-74 (M = Mg, Co, Fe) (<2.2), UTSA-20a (1.5), NOTT-300a (2.3) and M'MOF-2a (3.3) except M'MOF-3a (33.2), SIFSIX-2-Cu-i (41.0) and SIFSIX-1-Cu (8.37).[11−13] Although the C_2H_2 uptake of HOF-21a is inferior to that of the state-of-the-art SIFSIX materials, it is still much higher than outperformer M'MOF-3a, and the overall performance of HOF-21a for C_2H_2/C_2H_4 is better than that of M'MOF-3a. Although several HOFs constructed by pure organic linkers have been reported for gas separation, HOF-1 is the only one exhibiting very good C_2H_2/C_2H_4 separation, as preliminarily confirmed by the gas sorption isotherms.[4e] Because HOF-1 displays gas sorption hysteresis at room temperature, we cannot make straightforward comparison with HOF-21a in terms of their C_2H_2/C_2H_4 separation performance.

To further examine the separation performance of HOF-21a and compare with MPM-1-TIFSIX, column breakthrough experiments were performed, in which binary C_2H_2/C_2H_4 (50:50, *v*/*v*) mixture was flowed at the same total flow-rate (0.20 cm^3/min) at 298 K and 1 bar over a packed column of the HOF-21a and MPM-1-TIFSIX, respectively. As shown in Figure 2d, the efficient separation of C_2H_2/C_2H_4 mixture gases through a column packed with HOF-21a can be obtained. Ethylene behaved a very fast elution through the packed bed at 4 min, whereas acetylene was retained below 40 ppm until 32 min and reached saturation at 110 min. The captured amounts of C_2H_2 and C_2H_4 were 0.31 mmol/g and 0.028 mmol/g, respectively, giving a separation factor of 11 for 50:50 C_2H_2/C_2H_4 mixture gases and enabling HOF-21a to be a potential high-performance material for real industrial ethylene separation application. In case of MPM-1-TIFSIX (see Figure 2d, red), C_2H_2 almost emerges at the same time with C_2H_4 from the column bed though the retention time of both gases was much longer than that observed on HOF-21a. The separation factor is found to be only 2 on basis of their captured amounts. This also indicates that HOF-21a has a much better separation performance than MPM-1-TIFSIX.

To investigate the C_2H_2 adsorption sites in HOF-21a, we performed high-resolution neutron powder diffraction measurements on C_2D_2-loaded samples of HOF-21a·C_2D_2 at 200 K. Data were collected on a blank HOF-21a sample first, and then the sample was charged with a predetermined amount of C_2D_2 gas molecules and measured again. The data of the fully activated, bare HOF-21a sample indicate that its crystal structure exhibits a slight lattice distortion from perfect orthorhombic crystal system, and the diffraction peaks can be in indexed to the monoclinic *C*2/*c* space group. On the basis of the SXRD structure of the as-synthesized crystal, we solved the structure of the fully activated HOF-21a using direct method and subsequently performed Rietveld structural refinement. Reasonably good fit was obtained (see Figure 3a). For the

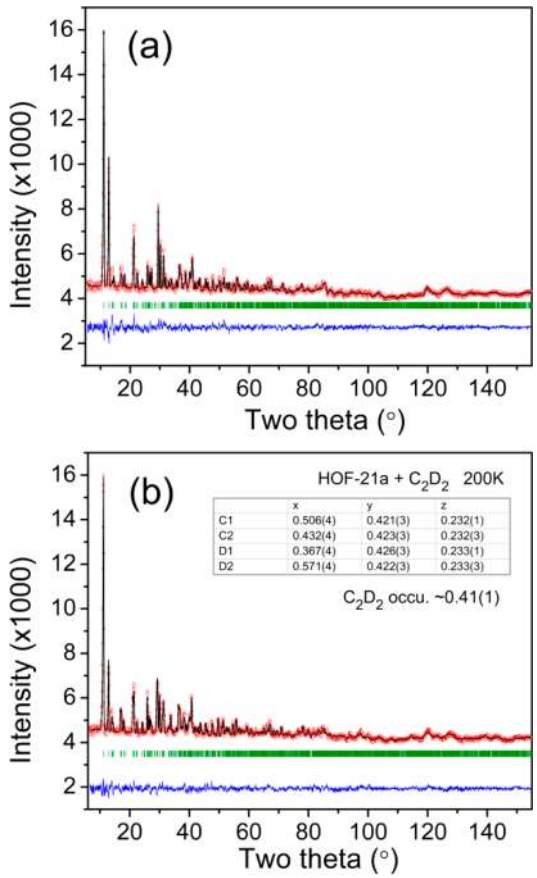

Figure 3. Rietveld refinements of the neutron powder diffraction data. Experimental (circles), calculated (line), and difference (line below observed and calculated patterns) neutron powder diffraction profiles for (a) HOF-21a and (b) HOF-21a loaded with C_2D_2, measured at 200 K, are shown. The adenine ligand molecules and C_2D_2 were kept as rigid bodies during the Rietveld structural refinement. Vertical bars indicate the calculated positions of Bragg peaks. For HOF-21a, goodness of fit data, R_{wp} = 0.0164, R_p = 0.0139, χ^2 = 1.201; for HOF-21a loaded with C_2D_2, goodness of fit data, R_{wp} = 0.0165, R_p = 0.0139, χ^2 = 1.216.

samples loaded with C_2D_2 molecules, Fourier difference analysis was conducted first to identify the gas molecule locations, and then full Rietveld structural refinement was carried out (see Figure 3b). The C_2D_2 adsorption configurations obtained from refinement are schematically shown in Figure 4a. The refined C_2D_2 concentration is ~0.41 C_2D_2 per building block unit, consistent with the experimental amount of gas loaded into the material. Clearly, the adsorbed C_2D_2 molecule (oriented in parallel to the crystallographic *a* axis) is bound to the F sites of two adjacent SiF_6 units with its D sites (see Figure 4a).

To further understand the C_2H_2 adsorption mechanism in HOF-21, we performed detailed computational investigations using first-principles DFT-D (dispersion-corrected density

DOI: 10.1021/jacs.7b13706
J. Am. Chem. Soc. 2018, 140, 4596−4603

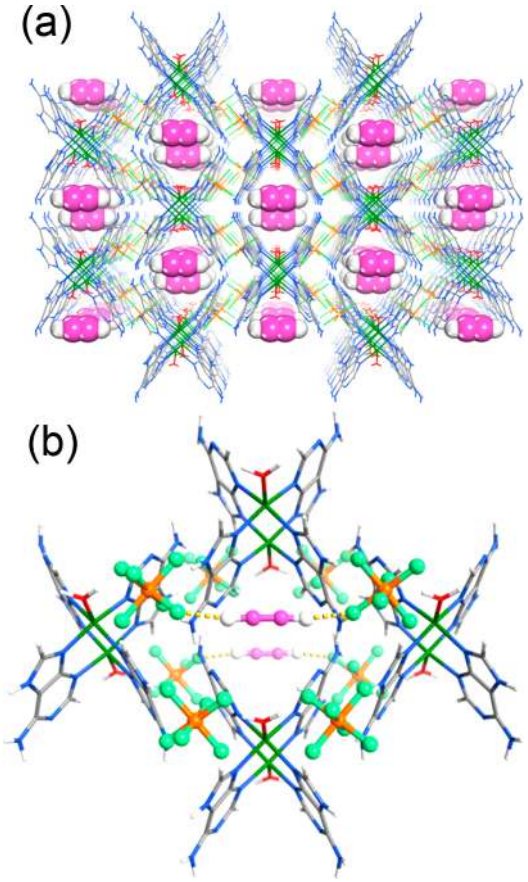

Figure 4. Neutron crystal structure of HOF-21a·C_2D_2 and DFT-D-calculated C_2H_2 adsorption sites of HOF-21a. (a) [001] view of the neutron crystal structure of HOF-21a·C_2D_2, determined from Rietveld analysis. The C_2D_2 molecules are shown in CPK method. (b) DFT-D-calculated C_2H_2 adsorption binding sites in HOF-21a. C_2H_2 interacts with the HOF-21a framework through "C−H···F" hydrogen bonding with SiF_6^{2-}. Si, orange; F, light green; N, blue; Cu, green; C on the ligand, gray, C on C_2D_2, pink; H/D, white.

functional theory) method. The optimized C_2H_2 adsorption locations and orientations are in full agreement with the experimental findings (see Figure 3b). C_2H_2 interacts with the HOF-21a framework through "C−H···F" hydrogen bonding, somewhat similar to the acetylene binding in SIFSIX MOFs recently reported by our group.[11] Note that in bare HOF-21a, all six F ions in the SiF_6 unit are already interacting with the hydrogen atoms in its neighboring adenine ligand, while in SIFSIX MOFs, the F sites available for gas adsorption are all uncoordinated terminal F sites. Therefore, single acetylene "C−H···F" hydrogen bond in HOF-21a is weaker than that in SIFSIX MOFs as indicated by the length of hydrogen bonding (2.215 Å in HOF-21a vs 2.017 Å in SIFSIX-1-Cu). In HOF-21a, however, each C_2H_2 molecule interacts with a SiF_6 unit on both ends and thus doubles the interaction strength (see Figure 4b). Indeed, the calculated static binding energy of C_2H_2 in HOF-21a is 45.1 kJ/mol, comparable to the C_2H_2 binding strength in typical SIFSIX-MOF materials (44.6 kJ/mol in SIFSIX-1-Cu). The static acetylene binding energy is somewhat larger than the experimental Q_{st} value but still reasonable, considering the difference in definition of the two and the accuracy limitation of the DFT-D approach.

In addition to selectivity, HOF-21 is thermally stable up to 353 K, evident by thermogravimetric analysis (see Figure S2). Practically, water stability is another very important factor when considering the porous materials for their practical adsorption applications. Considering the weak hydrogen bonding within HOFs, it seems to be a daunting challenge to establish HOFs with high water stability. Actually, most HOFs except HOF-8,[4j] MPM-1-TIFSIX,[6b] and SPA-1[6i] are very sensitive to water vapor, and hydrogen bonding network among the frameworks gradually collapses when exposed in air atmosphere. It seems impossible for them to survive in water. To confirm the stability of HOF-21a, the sample was first immersed into water for 24 h and then was examined its PXRD pattern. The PXRD pattern of the water-treated HOF-21a confirmed that HOF-21a was still stable under such harsh conditions (see Figure S1). As discussed above, the pore structure of HOF-21a can be maintained when evacuated at room temperature and temperature up to 353 K; however, it collapsed when it was evacuated under dynamic vacuum at higher temperature of 423 K, as confirmed from PXRD analysis (see Figure 5). This might be

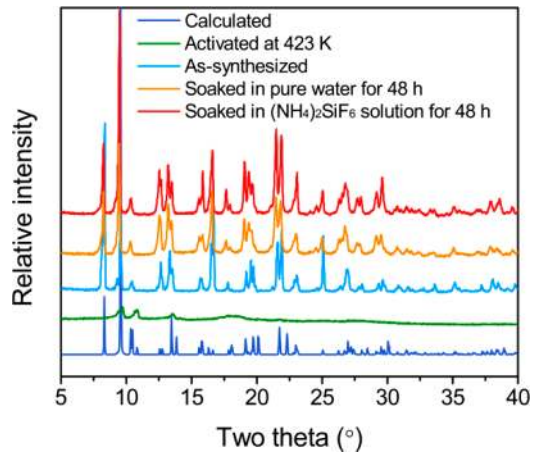

Figure 5. Structure recovery of HOF-21a. Comparison of the calculated PXRD pattern and those for the as-synthesized, collapsed, and restored HOF-21a from treatment in pure water and $(NH_4)_2SiF_6$ aqueous solution.

attributed to the loss of water molecule in axial positions. As water molecule in axial positions directly engaged in the formation of the whole hydrogen bonding network, the departure of water molecules can fluctuate or even break the structure of HOF-21a. Incredibly, by simply immersing the collapsed HOF-21a into water, the pore structures can be basically restored, as demonstrated by its gas sorption isotherm (see Figure S4) and PXRD patterns (see Figure 5). We suppose that water provides the necessary driving force to the self-assembly of HOF-21 since water plays an important role in structure stabilization by connecting to the adjacent units through hydrogen bonds (Figure 1c). On the other hand, the SiF_6^{2-} played a vital role in stabilizing the pore structure of HOF-21a, especially the multiple hydrogen-bonding interactions between the cationic $[Cu_2(ade)_4(H_2O)_2]^{4+}$ and SiF_6^{2-} anions. On the basis of such a speculation, we put the collapsed HOF-21a into water solution containing $(NH_4)_2SiF_6$ at room temperature for 48 h. Strikingly, the pore structures of HOF-21a can be restored almost completely, as indicated by the CO_2 gas sorption isotherm of salt-treated HOF-21a at 196 K (see Figure S4) and PXRD patterns (Figure 5). By comparison, it was clearly observed that MPM-TIFSIX could not recover when treated in the same manner (see Figures S5 and S6). It is

DOI: 10.1021/jacs.7b13706
J. Am. Chem. Soc. 2018, 140, 4596−4603

noteworthy that this is the first example of HOFs that can be easily recovered by simply immersing it into water or aqueous salt solution. As we have already known, the collapsed MOFs can be hardly recovered back into the porous frameworks in water or aqueous solutions. This superior property of HOF-21a in water is significantly important for its practical industrial applications.

CONCLUSION

In summary, we have realized a microporous hydrogen-bonded metal-complex or metallotecton framework HOF-21 with permanent porosity, which shows highly selective separation performance of C_2H_2/C_2H_4 at room temperature. The outstanding separation performance can be ascribed to the superimposed hydrogen-bonding interaction between C_2H_2 and SiF_6^{2-} on both ends, which is validated by modeling and neutron powder diffraction studies. HOF-21 combined the specialty of both MOFs and HOFs by introducing the metal-complex units to the hydrogen bonding network and enabling it with thermal and extreme water stability. More importantly, the collapsed HOF-21 can be recovered back to its original structure by simply immersing it into water or aqueous solution of anion source. To the best of our knowledge, such extraordinary water stability of HOF-21, meanwhile restorability, was observed for the first time in HOFs, highlighting the bright perspective of such new special HOF materials for practical industrial application.

ASSOCIATED CONTENT

Supporting Information

The Supporting Information is available free of charge on the ACS Publications website at DOI: 10.1021/jacs.7b13706.

XRD, BET, TGA, results of DFT calculations, dual sites Langmuir−Freundlich isotherm model fitting, isosteric heat of adsorption calculation (PDF)

Crystallographic file of HOF-21 (CIF)

Crystallographic file of HOF-21a (CIF)

AUTHOR INFORMATION

Corresponding Authors

*renql@zju.edu.cn

*banglin.chen@utsa.edu

*wzhou@nist.gov

ORCID

Hui Wu: 0000-0003-0296-5204

Wei Zhou: 0000-0002-5461-3617

Zhiguo Zhang: 0000-0003-1681-4853

Huabin Xing: 0000-0002-7418-0046

Michael J. Zaworotko: 0000-0002-1360-540X

Banglin Chen: 0000-0001-8707-8115

Notes

The authors declare no competing financial interest.

ACKNOWLEDGMENTS

This work was supported by National Key R&D Program of China (No. 2016YFB0301500), Zhejiang Provincial Natural Science Foundation of China (LR17B060001), National Natural Science Foundation of China (Nos. 21722609 and 21436010), Welch Foundation (AX-1730), and National Science Foundation (DMR-1606826).

REFERENCES

(1) (a) Sholl, D. S.; Lively, R. P. *Nature* **2016**, *532*, 435. (b) Nugent, P.; Belmabkhout, Y.; Burd, S. D.; Cairns, A. J.; Luebke, R.; Forrest, K.; Pham, T.; Ma, S.; Space, B.; Wojtas, L.; Eddaoudi, M.; Zaworotko, M. J. *Nature* **2013**, *495* (7439), 80. (c) Cui, Y.; Li, B.; He, H.; Zhou, W.; Chen, B.; Qian, G. *Acc. Chem. Res.* **2016**, *49* (3), 483. (d) Wu, H.; Gong, Q.; Olson, D. H.; Li, J. *Chem. Rev.* **2012**, *112* (2), 836.

(2) (a) Furukawa, H.; Cordova, K. E.; O'Keeffe, M.; Yaghi, O. M. *Science* **2013**, *341*, 1230444. (b) Liao, P. Q.; Zhang, W. X.; Zhang, J. P.; Chen, X. M. *Nat. Commun.* **2015**, *6*, 8697. (c) Matsuda, R.; Kitaura, R.; Kitagawa, S.; Kubota, Y.; Belosludov, R. V.; Kobayashi, T. C.; Sakamoto, H.; Chiba, T.; Takata, M.; Kawazoe, Y.; Mita, Y. *Nature* **2005**, *436* (7048), 238. (d) Sumida, K.; Rogow, D. L.; Mason, J. A.; McDonald, T. M.; Bloch, E. D.; Herm, Z. R.; Bae, T. H.; Long, J. R. *Chem. Rev.* **2012**, *112* (2), 724. (e) Zhai, Q. G.; Bu, X.; Zhao, X.; Li, D. S.; Feng, P. *Acc. Chem. Res.* **2017**, *50* (2), 407. (f) Yang, Q.; Liu, D.; Zhong, C.; Li, J. R. *Chem. Rev.* **2013**, *113* (10), 8261.

(3) (a) Feng, X.; Ding, X.; Jiang, D. *Chem. Soc. Rev.* **2012**, *41* (18), 6010. (b) Xu, H.; Gao, J.; Jiang, D. *Nat. Chem.* **2015**, *7* (11), 905.

(4) (a) Hu, F.; Liu, C.; Wu, M.; Pang, J.; Jiang, F.; Yuan, D.; Hong, M. *Angew. Chem., Int. Ed.* **2017**, *56* (8), 2101. (b) Ananchenko, G. S.; Moudrakovski, I. L.; Coleman, A. W.; Ripmeester, J. A. *Angew. Chem., Int. Ed.* **2008**, *47* (30), 5616. (c) Chen, T. H.; Popov, I.; Kaveevivitchai, W.; Chuang, Y. C.; Chen, Y. S.; Daugulis, O.; Jacobson, A. J.; Miljanic, O. S. *Nat. Commun.* **2014**, *5*, 5131. (d) Dalapati, S.; Saha, R.; Jana, S.; Patra, A. K.; Bhaumik, A.; Kumar, S.; Guchhait, N. *Angew. Chem., Int. Ed.* **2012**, *51* (50), 12534. (e) He, Y.; Xiang, S.; Chen, B. *J. Am. Chem. Soc.* **2011**, *133* (37), 14570. (f) Hisaki, I.; Nakagawa, S.; Tohnai, N.; Miyata, M. *Angew. Chem., Int. Ed.* **2015**, *54* (10), 3008. (g) Li, P.; He, Y.; Zhao, Y.; Weng, L.; Wang, H.; Krishna, R.; Wu, H.; Zhou, W.; O'Keeffe, M.; Han, Y.; Chen, B. *Angew. Chem., Int. Ed.* **2015**, *54* (2), 574. (h) Li, P.; He, Y.; Arman, H. D.; Krishna, R.; Wang, H.; Weng, L.; Chen, B. *Chem. Commun. (Cambridge, U. K.)* **2014**, *50* (86), 13081. (i) Lim, S.; Kim, H.; Selvapalam, N.; Kim, K. J.; Cho, S. J.; Seo, G.; Kim, K. *Angew. Chem., Int. Ed.* **2008**, *47* (18), 3352. (j) Luo, X. Z.; Jia, X. J.; Deng, J. H.; Zhong, J. L.; Liu, H. J.; Wang, K. J.; Zhong, D. C. *J. Am. Chem. Soc.* **2013**, *135* (32), 11684. (k) Sozzani, P.; Bracco, S.; Comotti, A.; Ferretti, L.; Simonutti, R. *Angew. Chem., Int. Ed.* **2005**, *44* (12), 1816. (l) Wang, H.; Li, B.; Wu, H.; Hu, T. L.; Yao, Z.; Zhou, W.; Xiang, S.; Chen, B. *J. Am. Chem. Soc.* **2015**, *137* (31), 9963. (m) Yang, W.; Greenaway, A.; Lin, X.; Matsuda, R.; Blake, A. J.; Wilson, C.; Lewis, W.; Hubberstey, P.; Kitagawa, S.; Champness, N. R.; Schröder, M. *J. Am. Chem. Soc.* **2010**, *132* (41), 14457. (n) Yang, W.; Li, B.; Wang, H.; Alduhaish, O.; Alfooty, K.; Zayed, M. A.; Li, P.; Arman, H. D.; Chen, B. *Cryst. Growth Des.* **2015**, *15* (4), 2000. (o) Zentner, C. A.; Lai, H. W.; Greenfield, J. T.; Wiscons, R. A.; Zeller, M.; Campana, C. F.; Talu, O.; FitzGerald, S. A.; Rowsell, J. L. *Chem. Commun. (Cambridge, U. K.)* **2015**, *51* (58), 11642. (p) Zhou, D. D.; Xu, Y. T.; Lin, R. B.; Mo, Z. W.; Zhang, W. X.; Zhang, J. P. *Chem. Commun. (Cambridge, U. K.)* **2016**, *52* (28), 4991. (q) Yadav, V. N.; Comotti, A.; Sozzani, P.; Bracco, S.; Bonge-Hansen, T.; Hennum, M.; Görbitz, C. H. *Angew. Chem., Int. Ed.* **2015**, *54* (52), 15684.

(5) (a) Das, M. C.; Xiang, S.; Zhang, Z.; Chen, B. *Angew. Chem., Int. Ed.* **2011**, *50* (45), 10510. (b) Das, M. C.; Guo, Q.; He, Y.; Kim, J.; Zhao, C. G.; Hong, K.; Xiang, S.; Zhang, Z.; Thomas, K. M.; Krishna, R.; Chen, B. *J. Am. Chem. Soc.* **2012**, *134* (20), 8703.

(6) (a) Dalrymple, S. A.; Shimizu, G. K. H. *J. Am. Chem. Soc.* **2007**, *129* (40), 12114. (b) Nugent, P. S.; Rhodus, V. L.; Pham, T.; Forrest, K.; Wojtas, L.; Space, B.; Zaworotko, M. J. *J. Am. Chem. Soc.* **2013**, *135* (30), 10950. (c) Thomas-Gipson, J.; Beobide, G.; Castillo, O.; Cepeda, J.; Luque, A.; Pérez-Yáñez, S.; Aguayo, A. T.; Román, P. *CrystEngComm* **2011**, *13* (10), 3301. (d) Thomas-Gipson, J.; Beobide, G.; Castillo, O.; Fröba, M.; Hoffmann, F.; Luque, A.; Pérez-Yáñez, S.; Román, P. *Cryst. Growth Des.* **2014**, *14* (8), 4019. (e) Thomas-Gipson, J.; Pérez-Aguirre, R.; Beobide, G.; Castillo, O.; Luque, A.; Pérez-Yáñez, S.; Román, P. *Cryst. Growth Des.* **2015**, *15* (2), 975. (f) Dechambenoit, P.; Ferlay, S.; Kyritsakas, N.; Hosseini, M. W. *J. Am. Chem. Soc.* **2008**, *130* (50), 17106. (g) Kawade, V. A.; Kumbhar,

DOI: 10.1021/jacs.7b13706
J. Am. Chem. Soc. 2018, 140, 4596−4603

A. S.; Erxleben, A.; Pachfule, P.; Banerjee, R. *CrystEngComm* **2011**, *13* (17), 5289. (h) Wang, C.-C.; Yeh, C.-T.; Cheng, Y.-T.; Chen, I. H.; Lee, G.-H.; Shih, W.-J.; Sheu, H.-S.; Fedorov, V. E. *CrystEngComm* **2012**, *14* (14), 4637. (i) Roques, N.; Mouchaham, G.; Duhayon, C.; Brandès, S.; Tachon, A.; Weber, G.; Bellat, J. P.; Sutter, J.-P. *Chem. - Eur. J.* **2014**, *20* (37), 11690. (j) Mouchaham, G.; Roques, N.; Khodja, W.; Duhayon, C.; Coppel, Y.; Brandès, S.; Fodor, T.; Meyer, M.; Sutter, J.-P. *Chem. - Eur. J.* **2017**, *23* (49), 11818. (k) Hamdouni, M.; Walha, S.; Duhayon, C.; Kabadou, A.; Sutter, J.-P. *CrystEngComm* **2017**, *19* (12), 1633. (l) Mouchaham, G.; Roques, N.; Kaiba, A.; Guionneau, P.; Sutter, J.-P. *CrystEngComm* **2010**, *12* (11), 3496. (m) Mouchaham, G.; Roques, N.; Brandès, S.; Duhayon, C.; Sutter, J.-P. *Cryst. Growth Des.* **2011**, *11* (12), 5424.

(7) Larson, A. C.; Von Dreele, R. B. *Los Alamos National Laboratory Report LAUR 86*; Los Alamos National Laboratory, 1994.

(8) Giannozzi, P.; Baroni, S.; Bonini, N.; Calandra, M.; Car, R.; Cavazzoni, C.; Ceresoli, D.; Chiarotti, G. L.; Cococcioni, M.; Dabo, I.; Dal Corso, A.; de Gironcoli, S.; Fabris, S.; Fratesi, G.; Gebauer, R.; Gerstmann, U.; Gougoussis, C.; Kokalj, A.; Lazzeri, M.; Martin-Samos, L.; Marzari, N.; Mauri, F.; Mazzarello, R.; Paolini, S.; Pasquarello, A.; Paulatto, L.; Sbraccia, C.; Scandolo, S.; Sclauzero, G.; Seitsonen, A. P.; Smogunov, A.; Umari, P.; Wentzcovitch, R. M. *J. Phys.: Condens. Matter* **2009**, *21* (39), 395502.

(9) Barone, V.; Casarin, M.; Forrer, D.; Pavone, M.; Sambi, M.; Vittadini, A. *J. Comput. Chem.* **2009**, *30* (6), 934.

(10) (a) Li, P.; He, Y.; Guang, J.; Weng, L.; Zhao, J. C.; Xiang, S.; Chen, B. *J. Am. Chem. Soc.* **2014**, *136* (2), 547. (b) Lu, J.; Perez-Krap, C.; Suyetin, M.; Alsmail, N. H.; Yan, Y.; Yang, S.; Lewis, W.; Bichoutskaia, E.; Tang, C. C.; Blake, A. J.; Cao, R.; Schroder, M. *J. Am. Chem. Soc.* **2014**, *136* (37), 12828. (c) Maji, T. K.; Matsuda, R.; Kitagawa, S. *Nat. Mater.* **2007**, *6* (2), 142. (d) Ok, K. M.; Sung, J.; Hu, G.; Jacobs, R. M. J.; O'Hare, D. *J. Am. Chem. Soc.* **2008**, *130* (12), 3762.

(11) Cui, X.; Chen, K.; Xing, H.; Yang, Q.; Krishna, R.; Bao, Z.; Wu, H.; Zhou, W.; Dong, X.; Han, Y.; Li, B.; Ren, Q.; Zaworotko, M. J.; Chen, B. *Science* **2016**, *353* (6295), 141.

(12) He, Y.; Krishna, R.; Chen, B. *Energy Environ. Sci.* **2012**, *5* (10), 9107.

(13) (a) Hu, T. L.; Wang, H.; Li, B.; Krishna, R.; Wu, H.; Zhou, W.; Zhao, Y.; Han, Y.; Wang, X.; Zhu, W.; Yao, Z.; Xiang, S.; Chen, B. *Nat. Commun.* **2015**, *6*, 7328. (b) Xiang, S. C.; Zhang, Z.; Zhao, C. G.; Hong, K.; Zhao, X.; Ding, D. R.; Xie, M. H.; Wu, C. D.; Das, M. C.; Gill, R.; Thomas, K. M.; Chen, B. *Nat. Commun.* **2011**, *2*, 204. (c) Yang, S.; Ramirez-Cuesta, A. J.; Newby, R.; Garcia-Sakai, V.; Manuel, P.; Callear, S. K.; Campbell, S. I.; Tang, C. C.; Schröder, M. *Nat. Chem.* **2015**, *7*, 121.

DOI: 10.1021/jacs.7b13706
J. Am. Chem. Soc. 2018, 140, 4596−4603